

Role of core excitation in (d,p) transfer reactions

A. Deltuva,¹ A. Ross,^{2,3} E. Norvaišas,¹ and F. M. Nunes^{2,3}

¹*Institute of Theoretical Physics and Astronomy,*

Vilnius University, Saulėtekio al. 3, LT-10222 Vilnius, Lithuania

²*National Superconducting Cyclotron Laboratory, Michigan State University, East Lansing, MI 48824, USA*

³*Department of Physics and Astronomy, Michigan State University, East Lansing, MI 48824-1321*

(Dated: October 25, 2021)

Background: Recent work found that core excitation can be important in extracting structure information from (d,p) reactions.

Purpose: Our objective is to systematically explore the role of core excitation in (d,p) reactions, and understand the origin of the dynamical effects.

Method: Based on the particle-rotor model of $n+^{10}\text{Be}$, we generate a number of models with a range of separation energies ($S_n = 0.1 - 5.0$ MeV), while maintaining a significant core excited component. We then apply the latest extension of the momentum-space based Faddeev method, including dynamical core excitation in the reaction mechanism to all orders, to the $^{10}\text{Be}(\text{d,p})^{11}\text{Be}$ like reactions, and study the excitation effects for beam energies from $E_d = 15 - 90$ MeV.

Results: We study the resulting angular distributions and the differences between the spectroscopic factor that would be extracted from the cross sections, when including dynamical core excitation in the reaction, to that of the original structure model. We also explore how different partial waves affect the final cross section.

Conclusions: Our results show a strong beam energy dependence of the extracted spectroscopic factors that become smaller for intermediate beam energies. This dependence increases for loosely bound systems.

PACS numbers: 21.10.Jx, 24.10.Ht, 25.40.Cm, 25.45.Hi

Keywords: (d,p) reactions, transfer reactions, core excitation

I. INTRODUCTION

Throughout the history of nuclear physics, transfer reactions have been important probes for nuclear structure and nuclear astrophysics. Within this broad class, $A(\text{d,p})B$ reactions play a prominent role due to the low Coulomb barrier and the well controlled description of the deuteron. In the last two decades, (d,p) reactions in inverse kinematics have been used to study properties of rare isotopes. One example is the study of the one-neutron halo nucleus ^{11}Be ; e.g. [1–4].

It is often the case that reaction theories freeze the degrees of freedom in the core, and consider only the static effects of core excitation by comparing the experimental cross sections with the reaction theory predictions assuming a single particle structure (e.g. [4]). This is done mostly for simplicity because the inclusion of core excitation represents a large increase in complexity and sometimes poses conceptual issues in the interpretation of data [5]. One may expect core excitation to come into play at some point, but it is unclear under what conditions these effects would be stronger. One may argue that at very high energies, the collision time is too short for dynamical effects, and that at very low energies, near and below the Coulomb barrier, there is less probability for the core to be excited. What happens in between these extreme limits is unclear. This is the topic we explore in the present paper.

Core excitation effects have been considered in detail in the context of the breakup of loosely bound two-body-like projectiles. The three-body continuum discretized coupled channel method has been extended to include

core excitation to all orders and a variety of applications [6–12] have all demonstrated that when including core excitation dynamically in the reaction, breakup observables are significantly modified. In some cases, the inclusion of core excitation helped describe specific features of the data or even modified the physical interpretation (e.g. [12]).

Recently, the full Faddeev formalism of [13] was extended to include core excitation [14, 15]. In [15], the method is applied to $^{10}\text{Be}(\text{d,p})^{11}\text{Be}$ and it is shown that dynamical core excitation can be very important for the reaction populating the ground state of ^{11}Be , while less important for that populating the first excited state. These results called for further study.

In this work, we will use the method developed in [15] and investigate the causes for the strong dynamical effects found in that work. We are particularly interested in exploring the dependence on the neutron separation energy and whether this is a phenomenon unique to halo nuclei. Although the purpose of our work is not to describe data, by isolating the specific features that induce the large core excitation effects, our work will help identify those experiments for which a more computationally intensive analysis, fully including core excitation in the reaction mechanism, may be needed.

The paper is organized as follows. In Section II we provide a brief description of the theory and the inputs required. Section III includes all our results, from the $n+^{10}\text{Be}$ toy models generated (Section IIIa), to angular distributions for elastic, inelastic and transfer cross sections (Section IIIb) and the resulting extracted structure information (Section IIIc). Finally, in Section IV we

present our summary and conclusions.

II. BRIEF DESCRIPTION OF THEORY AND INPUTS USED

The Faddeev formalism for the description of three-body nuclear reactions including core excitation and its numerical implementation is taken over from Ref. [15]. It is based on the integral form of the scattering theory as given by the Alt-Grassberger-Sandhas (AGS) equations [16] for three-body transition operators, extended for a multicomponent system, i.e.,

$$U_{\beta\alpha}^{ji} = \bar{\delta}_{\beta\alpha} G_0^{-1} + \sum_{\gamma=1}^3 \sum_{k=g,x} \bar{\delta}_{\beta\gamma} T_{\gamma}^{jk} G_0 U_{\gamma\alpha}^{ki}. \quad (1)$$

The subscripts α, β, γ label the spectator particles (interacting pairs in the odd-man-out notation), while the superscripts i, j, k label the components of the operators coupling different states of the core. Furthermore, $\bar{\delta}_{\beta\alpha} = 1 - \delta_{\beta\alpha}$, $G_0 = (E + i0 - H_0)^{-1}$ is the free resolvent at the reaction energy E , and

$$T_{\gamma}^{ji} = v_{\gamma}^{ji} + \sum_{k=g,x} v_{\gamma}^{jk} G_0 T_{\gamma}^{ki} \quad (2)$$

are two-body transition operators. The problem is formulated in an extended Hilbert space with two sectors corresponding to ground (g) and excited (x) states of the core. These two sectors are coupled by pairwise potentials v_{γ}^{ji} , while the extended free Hamiltonian H_0 is diagonal in the two sectors. Note that the kinetic energy operator also contains the internal core Hamiltonian. As a consequence, two- and three-body transition operators couple the two sectors as well. The amplitudes for three-body reactions are given by the on-shell matrix elements of $U_{\beta\alpha}^{ji}$ calculated between initial and final channel states $|\Phi_{\alpha}^i\rangle$. Denoting the core as particle 1 and proton as particle 2, amplitudes for elastic deuteron scattering are given by $\langle \Phi_1^g | U_{11}^{gg} | \Phi_1^g \rangle$, for inelastic deuteron scattering by $\langle \Phi_1^x | U_{11}^{xg} | \Phi_1^g \rangle$, and for the transfer reaction by $\langle \Phi_2^g | U_{21}^{gg} | \Phi_1^g \rangle + \langle \Phi_2^x | U_{21}^{xg} | \Phi_1^g \rangle$, since for the latter the final channel has two components.

Calculations are performed in momentum-space partial-wave representation. The proton-core Coulomb interaction is included via the screening and renormalization method [17]. Except for the partial waves with ^{11}Be bound states, described in details in the next section, the pair interactions v_{γ}^{ji} are chosen following the strategy of Ref. [15]. A realistic CD Bonn potential [18] is used for the np pair, acting in partial waves with pair orbital angular momentum $L \leq 3$. Nucleon-core potentials are based on the Chapel Hill 89 (CH89) parametrization [19], but are deformed with quadrupole deformation parameter $\beta_2 = 0.67$ and deformation length $\delta_2 = 1.664$ fm. As in Ref. [15], a subtraction technique is used to preserve the elastic nucleon-core cross section. The proton-core

(neutron-core) interaction is included in partial waves with pair orbital angular momentum $L \leq 10$ ($L \leq 5$). The total three-body angular momentum is limited to $J \leq 25$ which is sufficient for the convergence of elastic, inelastic and transfer observables.

III. RESULTS

A. Models for ^{11}Be

The three-body Faddeev method of [15] assumes the final nucleus can be represented within the particle-rotor model [20–22]. In this way, the ground state of a nucleus like ^{11}Be , would contain not only the $s_{1/2}$ components coupled to the ^{10}Be ground state, but also $d_{3/2}$ and $d_{5/2}$ components coupled to the ^{10}Be 2^+ first excited state (with excitation energy of $E_x = 3.368$ MeV), resulting from the quadrupole deformation of the core ^{10}Be . It is widely accepted that, indeed, the ground state of ^{11}Be contains a $\approx 20\%$ core excited d-wave admixture in the wavefunction.

To explore core excitation effects and its dependence on the neutron separation energy, we needed to generate a variety of $n+^{10}\text{Be}$ models. Starting from the model developed in [21] one can produce a variety of models with different separation energies just by changing the depth of the central interaction while keeping the geometry fixed. It is important to ensure that all models produce a similar significant admixture as the original ^{11}Be model of [21]. If the $n+^{10}\text{Be}$ system exhibits a larger core excited component one might induce larger core excitation effects in the reaction as a consequence of the structure, rather than the reaction mechanism. While most models include a core with the physical excitation energy of the 2^+ state in ^{10}Be , we also explored the effect of a small excitation energy $E_x = 0.5$ MeV. There are a couple of $n+^{10}\text{Be}$ models in Table I developed for this purpose.

The resulting potentials are presented in Table I. We include the central depth V_{ws} , the spin-orbit depth V_{so} , the deformation length $\delta_2 = \beta_2 R_{ws}$ and the core 2^+ excitation energy E_x . The geometry of the central and spin-orbit force are kept as in [21], namely $R_{ws} = 2.483$ fm, $a_{ws} = 0.65$ fm. The last two columns in Table I correspond to the percent probability associated with the dominant partial waves included in the $n+^{10}\text{Be}$ model space (also referred to as the theoretical spectroscopic factors). These results were obtained with EFADDY [23] by solving the coupled channel equation [20], but were verified also by momentum-space calculations.

For comparing the core excitation results with those obtained under the assumption of a single-particle structure, we also produce the corresponding $n+^{10}\text{Be}$ single-particle potentials. Here we have imposed volume conservation as discussed in [20]. The central depths of the resulting potentials are summarized in Table II.

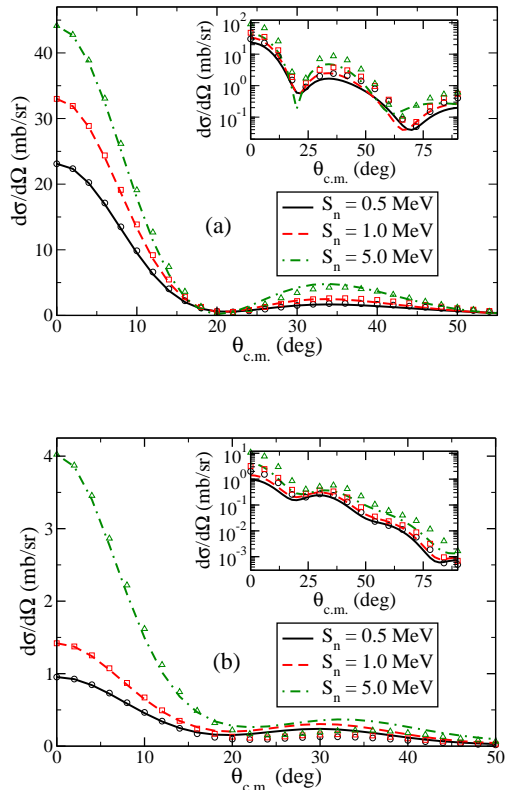


FIG. 1: (Color online) Angular distributions for $^{10}\text{Be}(d,p)^{11}\text{Be}(g.s.)$ at 20 MeV (a) and 80 MeV (b) for various separation energies of the final nucleus.

B. Predicted cross sections

The magnitude of the transfer cross sections depends strongly on the beam energy and their angular distribution provides information on the internal orbital angular momentum of the final nucleus. For a given beam energy, the transfer cross section is largest when there is optimum Q-value matching. In Figs.1(a) and (b) we show the angular distributions for $^{10}\text{Be}(d,p)^{11}\text{Be}$ for deuteron energies of 20 MeV and 80 MeV, respectively, produced with

S_n (MeV)	V_{ws} (MeV)	V_{so} (MeV)	δ (fm)	E_x (MeV)	$S_{s1/2}^{th}$	$S_{d5/2}^{th}$
0.1	-51.924	-8.5	1.664	3.368	94.2	5.4
0.5	-54.45	-8.5	1.664	3.368	85.4	12.5
0.5	-52.988	-1.0	1.664	0.500	79.2	13.3
1.0	-56.475	-8.5	1.664	3.368	78.7	18.4
5.0	-67.059	-8.5	1.664	3.368	57.7	37.4
5.0	-65.670	-1.0	1.664	0.500	54.5	29.7

TABLE I: Parameters for the $n+^{10}\text{Be}$ system taking into account the $^{10}\text{Be}(2^+)$ core excitation, and the resulting spectroscopic factors, as a function of the neutron separation energy S_n .

the full Faddeev method including core excitation: the solid black line represents the prediction for the model with the realistic separation energy, while the red-dashed and the green-dot-dashed correspond to a separation energy of $S_n = 1$ MeV and $S_n = 5$ MeV, respectively. The distributions are all forward peaked because they correspond to $L = 0$ transitions. The insets in Figs.1(a) and (b) correspond to the same data but instead in log plot. In addition to the predictions including fully dynamical core excitation, we include, in symbols, the predictions obtained neglecting core excitation (circles for $S_n = 0.5$ MeV, squares for $S_n = 1$ MeV and triangles for $S_n = 5$ MeV).

Focusing now on the log plots of Figs.1 (a) and (b), the main effect of core excitation is to reduce the cross section. This is reflected in the fact that the normalizations needed to match the single-particle predictions with the core excited predictions are smaller than unity. For example, for $S_n = 0.5$ MeV, the normalization needed for the single-particle cross sections for $E_d = 20$ MeV is $SF = 0.76$, while for $E_d = 80$ MeV it is $SF = 0.48$. We will come back to this discussion in Section III C.

In the linear plots only, the single-particle predictions have been normalized by an arbitrary factor to match the full core excited predictions at zero degrees, to make the comparison of the shapes of the distributions easier. At low beam energies, minor changes in the shape of the angular distribution are seen. However at the higher energies there is a significant change in the shape for larger angles.

The nucleon-target interactions determine the details of the elastic and inelastic distributions. In the full Faddeev calculations, these predictions are produced consistently with the transfer predictions. For completeness, we show in Fig.2 the elastic and inelastic cross sections as functions of scattering angle for $E_d = 20$ MeV and $E_d = 80$ MeV. The full Faddeev predictions with core excitation are shown by the lines: solid black line for $S_n = 0.5$ MeV, dashed red line for $S_n = 1$ MeV, and green dot-dashed line for $S_n = 5$ MeV. The plots for the elastic distributions also contain the single-particle predictions in symbols (black circles for $S_n = 0.5$ MeV, red squares for $S_n = 1$ MeV, and green triangles for $S_n = 5$ MeV). The elastic distribution is not very sensitive to the separation energy of the system, but we see that the inelastic cross section decreases with increasing separa-

S_n (MeV)	V_{ws} (MeV)
0.1	-57.319
0.5	-61.243
1.0	-64.337
5.0	-79.378

TABLE II: Single particle parameters for $n+^{10}\text{Be}$ system, as a function of the neutron separation energy S_n . The depth of the spin-orbit force is the same for all these models $V_{so} = 8.5$ MeV.

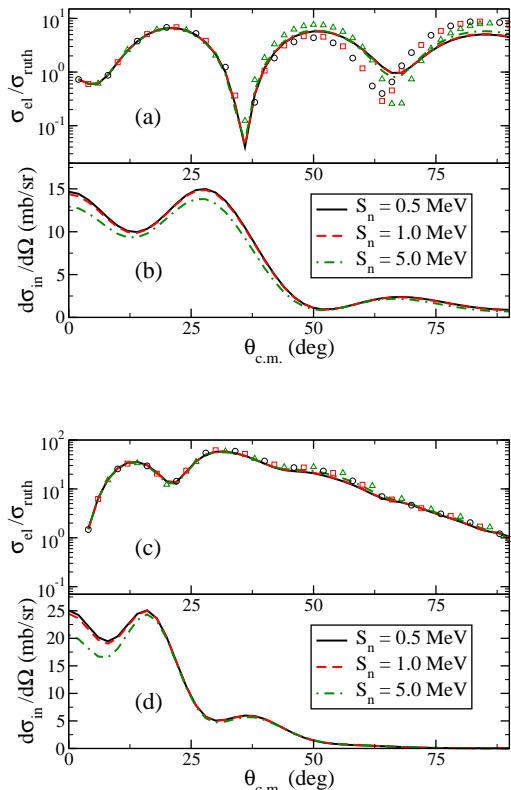


FIG. 2: (Color online) Angular distributions for $^{10}\text{Be}(d,d)^{10}\text{Be}$ (ratio to Rutherford) and $^{10}\text{Be}(d,d')^{10}\text{Be}^{2+}$ at 20 MeV (a) and (b) and 80 MeV (c) and (d): Faddeev predictions are obtained for various separation energies of the final nucleus in the (d,p) transfer channel.

tion energy, a consequence of the fact that the transition operator is mostly sensitive to the surface of the optical potential (the operator is roughly proportional to the derivative of the optical potential) and therefore is enhanced when the composite nucleus has large tails (small separation energies). Note that the single-particle model predicts no inelastic cross sections. An experiment that measures all three channels (elastic, inelastic and transfer) simultaneously will provide stringent constraints to the reaction model.

Of course, in addition, the Faddeev method with core excitation also predicts elastic breakup cross sections (which leave ^{10}Be in its ground state) and inelastic breakup cross sections (which leave ^{10}Be in its 2^+ excited state). However, it is far more demanding to obtain convergence for these observables and it is beyond the scope of this work.

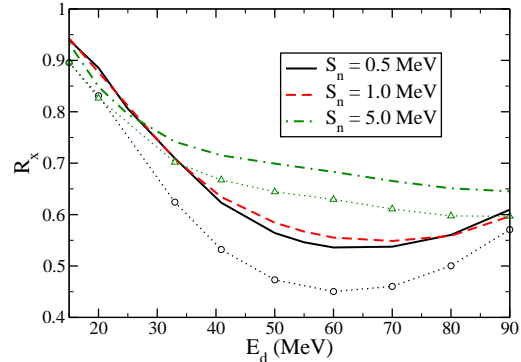


FIG. 3: (Color online) Spectroscopic factor ratio R_x as a function of the beam energy extracted from $^{10}\text{Be}(d,p)^{11}\text{Be}$ for various separation energies of the final nucleus (more details in the text).

C. Extracted structure information

Often (d,p) transfer experiments are performed with the objective of extracting a spectroscopic factor. This is done by taking the ratio of the measured cross section at the peak of the angular distribution and the corresponding theoretical prediction, assuming a pure single-particle final state: $S^{exp} = \frac{d\sigma^{exp}}{d\Omega} / \frac{d\sigma^{sp}}{d\Omega}$. Let us consider specifically the realistic case of $^{10}\text{Be}(d,p)^{11}\text{Be}$. We understand that the realistic overlap function for the ground state of ^{11}Be has in addition to the neutron $s_{1/2}$ wave coupled to $^{10}\text{Be}(0^+)$, components where the core is excited (in our model only $^{10}\text{Be}(2^+)$ is considered). Due to the excitation energy of the core $E_x = 3.368$ MeV, the tails of the overlap function for those core-excited components die off much faster than the $s_{1/2}$ component, which has an exponential decay dominated by $S_n = 0.5$ MeV. For that reason, it is this $s_{1/2}$ component that dominates the final cross section. If no dynamical core excitation takes place during the reaction, then the ratio of cross sections S^{exp} corresponds exactly to $S_{s_{1/2}}^{th}$, the probability that the valence neutron is indeed in the $s_{1/2}$ single-particle orbital in the ^{11}Be -like system. However, dynamical effects in the reaction can change this value and produce erroneous conclusions when extracting the spectroscopic factor from transfer angular distributions.

We test this idea using the full Faddeev predictions which include core excitation to all orders. These predictions serve as our data and, by comparing them with the single particle predictions, we can extract S^{Fadd} as a ratio of the Faddeev cross section when core excitation is included and the single-particle Faddeev prediction, i.e., $S^{Fadd} = \frac{d\sigma^{ceex}}{d\Omega} / \frac{d\sigma^{sp}}{d\Omega}$. We then take the ratio of this spectroscopic factor S^{Fadd} and the spectroscopic factor $S_{s_{1/2}}^{th}$ introduced in our ^{11}Be structure model (Table I). This quantity is defined as $R_x = S^{Fadd} / S_{s_{1/2}}^{th}$ and is plotted

in Fig. 3 for several separation energies as a function of beam energy: $S_n = 0.5$ MeV (solid black), $S_n = 1$ MeV (dashed red) and $S_n = 5$ MeV (dot-dashed green). If there were no dynamical excitations in the reaction, R_x should be unity, independent of the beam energy. We find that R_x is not unity and depends strongly on beam energy as was already indicated in [15].

The coupling between components with different core states (in this case a quadrupole term) is peaked at the surface; as mentioned before the operator is roughly the derivative of the optical potential. For cases in which the neutron separation energy is considerably smaller than the excitation energy, one might naively expect two limiting cases: at very small beam energies, dynamical effects should be small because the Coulomb barrier keeps the deuteron far from the target not allowing the nuclear quadrupole coupling to act, and at very high beam energies, dynamical effects should also decrease because the timescale for the reaction hinders multistep effects. It is for intermediate beam energies that one can expect dynamical effects to take place. This is exactly what is seen in Fig. 3. Unfortunately there are numerical difficulties in obtaining converged Faddeev calculations for beam energies lower than $E_d = 15$ MeV. The solid line starts at $R_x = 0.94$ for $E_d = 15$ MeV, which is well above the Coulomb barrier. It then decreases to a maximum effect around $E_d = 60 - 70$ MeV ($R_x = 0.54$), raising again for the higher beam energies. Extracting a spectroscopic factor from data in the range $E_d = 40 - 90$ MeV using the single-particle predictions can lead to very large underprediction of the spectroscopic factor.

Fig. 3 also shows that the effect of dynamical core excitation is more pronounced for the more loosely bound systems. This result appears at first counter intuitive: if the transferred neutron moves into a loosely bound orbital, it may not feel the effects of core excitation as much. This is not the case: the larger the separation energy, the smaller the strength of the coupling to excited states (due to a weaker overlap of the ^{11}Be -like components and the transition operator). This manifests as a weaker dependence of R_x as a function of beam energy. Although the dynamical effects described by the full Faddeev equations are highly non-linear, we found that the dependence of R_x on the separation energy S_n is approximately linear except when the separation energy approaches zero. The value of the separation energy for this change in behavior depends on E_d (for example, at $E_d = 41$ MeV the linear behavior extends down to $S_n = 0.3$ MeV).

Reducing the excitation energy of the core, increases the overlap of the ^{11}Be -like core-excited components and the transition operator. In Fig. 3 we also show the predictions when $E_x = 0.5$ MeV. For both $S_n = 0.5$ MeV (black circles) and $S_n = 5$ MeV (green triangles), the dynamical effects of core excitation are enhanced when E_x decreases, as demonstrated by the fact that the extracted ratios $R_x(E_d)$ for $E_x = 0.5$ MeV are below the $R_x(E_d)$ lines corresponding to $E_x = 3.368$ MeV.

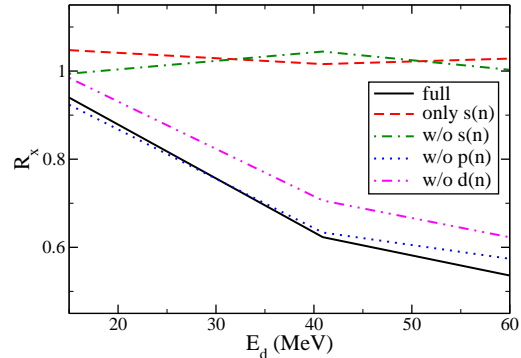


FIG. 4: (Color online) Spectroscopic factor ratio R_x as a function of beam energy extracted from $^{10}\text{Be}(d,p)^{11}\text{Be}$, switching off various couplings (see text for more detail).

If we just include core excitation in the ^{11}Be bound state, $R_x \approx 1$ for all beam energies, which demonstrates that breakup is critical to enable the dynamical effects we observe. We then investigate the different partial waves in the nucleon-target subsystem that are responsible for the effect. In Fig. 4 we show the predictions for R_x when only the s-wave is included in the neutron-target relative motion (dashed red line) and compare it to the results including all partial waves (solid black line). We see that including only s-wave in the neutron-target continuum produces virtually no effect. On the other hand, switching off the s-wave, while keeping all other components in the calculation (dot-dashed green line) also produces no effect. We also show the results obtained when switching off the p-wave (dotted blue line) and the d-wave (dot-dot-dashed purple line). It is the interplay of both s-waves and d-waves that causes the large reduction observed for R_x . We find that, for the proton-target interaction, many partial waves are needed for convergence but there is no strong interference between them, as for the neutron-target case.

In analogy with the previously studied nucleon-deuteron scattering including dynamically the Δ -isobar excitation [24], the core excitation effect can be separated into contributions of two- and three-body nature. Inclusion of only the two-body part is possible within standard AGS equations with effective transition operators acting in a single sector (g) of the Hilbert space. The results of this calculation typically go in the opposite direction as compared to the full calculation, thereby indicating that there is a strong competition between the contributions of two- and three-body nature, and the full core excitation effect is a result of a complicated interplay between them. These findings are in qualitative agreement with those of nucleon-deuteron scattering with the Δ -isobar excitation [24].

Our NN interaction is the full CD-Bonn which contains the tensor force and produces a deuteron bound state

with the appropriate d-wave component. Although we focused our study in the ^{11}Be structure, we also wanted to explore whether the NN tensor interaction could be contributing to the dynamical effects we observe. We repeated the calculations (including core excitation and assuming a single-particle structure) using a simple Gaussian interaction for the NN force in the deuteron partial wave (as in [25]). The R_x obtained in this way are within 2 % of those obtained with the full CD-Bonn. We thus conclude that the NN tensor force is not responsible for the dynamical effect under study.

IV. SUMMARY AND CONCLUSIONS

Our main goal in this work is to systematically explore the role of core excitation in (d,p) reactions, and understand the origin of the dynamical effects. We generate a number of two-body $n+^{10}\text{Be}$ models for a ^{11}Be -like system, with a range of neutron separation energies ($S_n = 0.1 - 5.0$ MeV), keeping a significant core excited component. We then perform full Faddeev calculations including core excitation to all orders to obtain elastic, inelastic and transfer cross sections. We study the effect of core excitation and extract the spectroscopic factor that would be obtained taking the ratio of the full calculation with that of the single-particle model, for a range of beam energies.

The spectroscopic factors obtained by taking this ratio do not agree with the spectroscopic factor in the original model. For example, in the case of the realistic ^{11}Be , the spectroscopic factor obtained is strongly dependent on beam energy, with a minimum of half its original value at intermediate beam energies of around 60 – 70 MeV. All this points towards the fact that dynamical core excitation is indeed distorting the results and should be explicitly included in the reaction mechanism for a reliable extraction of structure information. Increasing the neutron separation energy, reduces the effect.

In order to fully explore this dynamical effect we also

perform calculations when the excitation energy of the core is arbitrarily reduced to 0.5 MeV. This reduction increases the role of core excitation, regardless of the separation energy of the system, or the beam energy considered, since then the core excited components in the ^{11}Be -like system have an asymptotic fall-off comparable to the component where the core is in its ground state, enhancing core-excitation couplings.

Finally, we also explore the role of different partial waves in the nucleon-target subsystem in the final transfer cross section. We find that interference effects between s-wave and d-waves in the neutron-target continuum are essential to reproduce the full result.

This interesting phenomenon of dynamical core excitation is sufficiently large that it merits experimental investigation. The reaction $^{10}\text{Be}(d,p)^{11}\text{Be}$ has been measured in the lower energy regime [4]. Unfortunately the magnitude of the transfer cross section decreases significantly with beam energy. However, a measurement in the intermediate energy range $E_d = 80$ MeV may still be feasible and would provide a crucial test on the predictions of the reaction model, particularly if the various reaction channels are measured simultaneously as in [4].

A similar investigation of the role of core excitation in Eikonal models for nuclear knockout reactions and its dependence on beam energy may shed light on the reductions factor observed when extracting structure information from those measurements [26].

ACKNOWLEDGMENTS

We are grateful to Charlotte Elster for useful discussions. The work of A.D. and E.N. was supported by Lietuvos Mokslo Taryba (Research Council of Lithuania) under contract No. MIP-094/2015. The work of A.R. and F.M.N. was supported by the National Science Foundation under Grants No. PHY-1520929 and PHY-1403906 and the Department of Energy under Contract No. DE-FG52-08NA28552.

-
- [1] S. Fortier, S. Pita, J. Winfield, W. Catford, N. Orr, J. V. de Wiele, Y. Blumenfeld, R. Chapman, S. Chappell, N. Clarke, et al., *Physics Letters B* **461**, 22 (1999), ISSN 0370-2693, URL <http://www.sciencedirect.com/science/article/pii/S0370269399008254>.
 - [2] J. Winfield, S. Fortier, W. Catford, S. Pita, N. Orr, J. V. de Wiele, Y. Blumenfeld, R. Chapman, S. Chappell, N. Clarke, et al., *Nuclear Physics A* **683**, 48 (2001), ISSN 0375-9474, URL <http://www.sciencedirect.com/science/article/pii/S0375947400004632>.
 - [3] K. T. Schmitt, K. L. Jones, A. Bey, S. H. Ahn, D. W. Bardayan, J. C. Blackmon, S. M. Brown, K. Y. Chae, K. A. Chipps, J. A. Cizewski, et al., *Phys. Rev. Lett.* **108**, 192701 (2012).
 - [4] K. T. Schmitt, K. L. Jones, S. Ahn, D. W. Bardayan, A. Bey, J. C. Blackmon, S. M. Brown, K. Y. Chae, K. A. Chipps, J. A. Cizewski, et al., *Phys. Rev. C* **88**, 064612 (2013), URL <http://link.aps.org/doi/10.1103/PhysRevC.88.064612>.
 - [5] A. E. Lovell and F. M. Nunes, *Journal of Physics G: Nuclear and Particle Physics* **42**, 034014 (2015).
 - [6] N. C. Summers, F. M. Nunes, and I. J. Thompson, *Phys. Rev. C* **73**, 031603 (2006), URL <http://link.aps.org/doi/10.1103/PhysRevC.73.031603>.
 - [7] N. C. Summers, F. M. Nunes, and I. J. Thompson, *Phys. Rev. C* **74**, 014606 (2006), URL <http://link.aps.org/doi/10.1103/PhysRevC.74.014606>.
 - [8] N. C. Summers, F. M. Nunes, and I. J. Thompson, *Phys. Rev. C* **89**, 069901(E) (2014), URL <http://link.aps.org/doi/10.1103/PhysRevC.89.069901>.

- [9] N. C. Summers and F. M. Nunes, *Phys. Rev. C* **76**, 014611 (2007), URL <http://link.aps.org/doi/10.1103/PhysRevC.76.014611>.
- [10] N. C. Summers and F. M. Nunes, *Phys. Rev. C* **77**, 049901(E) (2008), URL <http://link.aps.org/doi/10.1103/PhysRevC.77.049901>.
- [11] A. M. Moro and J. A. Lay, *Phys. Rev. Lett.* **109**, 232502 (2012), URL <http://link.aps.org/doi/10.1103/PhysRevLett.109.232502>.
- [12] R. de Diego, J. M. Arias, J. A. Lay, and A. M. Moro, *Phys. Rev. C* **89**, 064609 (2014), URL <http://link.aps.org/doi/10.1103/PhysRevC.89.064609>.
- [13] A. Deltuva and A. C. Fonseca, *Phys. Rev. C* **79**, 014606 (2009), URL <http://link.aps.org/doi/10.1103/PhysRevC.79.014606>.
- [14] A. Deltuva, *Phys. Rev. C* **88**, 011601 (2013), URL <http://link.aps.org/doi/10.1103/PhysRevC.88.011601>.
- [15] A. Deltuva, *Phys. Rev. C* **91**, 024607 (2015), URL <http://link.aps.org/doi/10.1103/PhysRevC.91.024607>.
- [16] E. O. Alt, P. Grassberger, and W. Sandhas, *Nucl. Phys.* **B2**, 167 (1967).
- [17] A. Deltuva, A. C. Fonseca, and P. U. Sauer, *Phys. Rev. C* **71**, 054005 (2005).
- [18] R. Machleidt, *Phys. Rev. C* **63**, 024001 (2001).
- [19] R. Varner, W. Thompson, T. McAbee, E. Ludwig, and T. Clegg, *Physics Reports* **201**, 57 (1991), ISSN 0370-1573.
- [20] F. Nunes, I. Thompson, and R. Johnson, *Nuclear Physics A* **596**, 171 (1996), ISSN 0375-9474, URL <http://www.sciencedirect.com/science/article/pii/0375947495003983>.
- [21] F. Nunes, J. Christley, I. Thompson, R. Johnson, and V. Efros, *Nuclear Physics A* **609**, 43 (1996), ISSN 0375-9474, URL <http://www.sciencedirect.com/science/article/pii/0375947496002849>.
- [22] F. Nunes, Ph.D. thesis, University of Surrey (1995).
- [23] I.J. Thompson, V. D. Efros, and F. Nunes (2004), URL <http://www.fresco.org.uk/programs/efaddy/>.
- [24] A. Deltuva, R. Machleidt, and P. U. Sauer, *Phys. Rev. C* **68**, 024005 (2003).
- [25] N. J. Upadhyay, A. Deltuva, and F. M. Nunes, *Phys. Rev. C* **85**, 054621 (2012).
- [26] J. A. Tostevin and A. Gade, *Phys. Rev. C* **90**, 057602 (2014), URL <http://link.aps.org/doi/10.1103/PhysRevC.90.057602>.